Energy &
Environmental Science

RSCPublishing

COMMUNICATION

View Article Online
View Journal | View Issue

Cite this: *Energy Environ. Sci.*, 2013, **6**, 2907

Received 14th June 2013
Accepted 23rd July 2013

DOI: 10.1039/c3ee42001a

www.rsc.org/ees

Increasing the power output of a CdTe solar cell *via* luminescent down shifting molecules with intramolecular charge transfer and aggregation-induced emission characteristics†

Yilin Li,[ab] Zhipeng Li,[a] Yang Wang,‡[b] Alvin Compaan,[c] Tianhui Ren*[a] and Wen-Ji Dong*[b]

A series of tetraphenylethylene (TPE) based luminescent downing-shifting (LDS) molecules was synthesized based on a new design strategy for electron donor–acceptor conjugated fluorophores, in which TPE was paired with malononitrile and used as an electron donor. Because of their strong characteristics of intramolecular charge transfer (ICT) and aggregation-induced emission (AIE), the synthesized fluorophores exhibit both large Stokes shifts (129–146 nm) and high quantum yields (0.84–0.99). Applied PMMA solid films doped with the synthesized molecules on the surface of a CdTe solar cell can significantly increase its short circuit current density (J_{sc}) by a magnitude of 6–10%.

The cadmium telluride (CdTe) solar cell is considered one of the most promising PV technologies for a significant portion of the PV market in the future because of its low-cost and easy-manufacturing compared to the traditional crystalline silicon (c-Si) solar cell.[1] However, the spectral response of the CdTe solar cell exhibits a cut off in the short-wavelength region (<500 nm) where its external quantum efficiency (EQE) is less than 0.20 due to absorption of the cadmium sulfide (CdS) layer in the cell structure in this region. Such poor response at short-wavelengths limits the average module efficiency of the CdTe solar cell to around 12.6%.[2] One approach to improving the spectral response of the CdTe solar cell at short-wavelengths is to modify the spectrum of the incident light by placing a layer of a luminescent down-shifting (LDS) material on the cell surface, which can absorb the photons below 500 nm and re-emit them over 550 nm which is the strong spectral response region (EQE > 0.80) of the CdTe solar cell.[3,4] For effective spectral modification, three criteria are required for these LDS materials: (i) strong absorption in the region where the spectral response of the CdTe solar cell is weak, (ii) a close to unity quantum yield of emission in the region where the spectral response of the CdTe solar cell is strong, and (iii) a large Stokes shift separating the absorption and emission to minimize the photon self-absorption.

Broader context

The CdTe solar cell is one of today's widely used solar cells. Although it possesses the advantages of low-cost and easy-manufacturing, the relative low efficiency (average 12.6% at the module level) limits its broader applications compared to traditional crystalline silicon solar cells. One of the chief problems of low efficiency lies in the spectral mismatch with the solar spectrum. Its spectral response exhibits a cut off below 500 nm, with a relatively high response over 550 nm. Rather than optimizing the cell structure, the most effective way of addressing this issue is to use a layer of a luminescent down-shifting (LDS) material to convert the unfavorable photons (<500 nm) into favorable photons (>550 nm) before the incident light reaches the cell surface. In this study, a series of novel tetraphenylethylene-based LDS molecules were synthesized. These fluorophores were pre-designed to have both intramolecular charge transfer (ICT) and aggregation-induced emission (AIE) characteristics, which allows them to exhibit large Stokes shifts (129–146 nm) and high quantum yields (0.84–0.99) in the solid state. Fluorophore-doped PMMA solid films enhance the short-wavelength response of a CdTe solar cell and significantly increase its short circuit current density (J_{sc}) by a magnitude of 6–10%.

In an effort to search for effective LDS materials, a commercially available fluorophore BASF Lumogen F dye Yellow 083 (Y083) has been widely used to study the enhancement of the power output of the CdTe solar cell.[5–7] However, Y083 has a poor spectral response to the 300–400 nm UV light in its absorption spectrum.[8] Though it exhibits a high quantum yield ($\Phi_f = 0.92$), its emission spectrum mismatch with the spectral response of the CdTe solar cell decreases its spectral conversion efficiency. More importantly, when it is doped into a

---

[a] *School of Chemistry and Chemical Engineering, Shanghai Jiao Tong University, Shanghai 200240, China. E-mail: thren@sjtu.edu.cn; Tel: +86-21-54747118*

[b] *Voiland School of Chemical Engineering and Bioengineering, Washington State University, Pullman, WA 99164, USA. E-mail: wdong@vetmed.wsu.edu; Tel: +01-509-335-5798*

[c] *Department of Physics and Astronomy, The University of Toledo, Toledo, OH 43606, USA*

† Electronic supplementary information (ESI) available. See DOI: 10.1039/c3ee42001a

‡ Undergraduate summer intern from Department of Chemistry, University of California Berkeley.

solid film at high concentration, it shows some degree of aggregation-caused fluorescence quenching leading to decreased spectral conversion efficiency.[9]

The aggregation-caused fluorescence quenching at high concentration has been a common problem for many fluorophores that prevents them from being LDS materials for solar cell applications. However, it has been reported that some tetraphenylethylene (TPE) based donor–acceptor (D–A) type fluorophores can suppress the aggregation-caused fluorescence quenching by a mechanism of aggregation-induced emission (AIE).[10,11] On the one hand, most of these AIE fluorophores typically exhibit very high quantum yield in the solid state, but with maximum emission in the region below 500 nm.[12–14] This is primarily caused by the fact that the TPE group of these D–A type fluorophores always serves as an electron acceptor that dominates the molecular emission properties of the fluorophores.[15] On the other hand, some of the AIE fluorophores do show maximum emission in the region over 500 nm by extending the π-conjugated molecular structures,[16–18] but their fluorescence quantum yields are lower because of the extended π-conjugated molecular structures that promote electron movement and molecular vibration during the emission process, and therefore enhance non-radiative relaxation.[19] Because of these unfavorable photonic properties, these AIE fluorophores are poor candidates as LDS materials for CdTe solar cell applications.

To take advantage of the AIE mechanism and explore the potential application of AIE fluorophores in solar energy harvesting using a CdTe solar cell, in this communication, we report a type of newly designed and synthesized TPE-based AIE fluorophore in which the TPE group acts as an electron donor in the presence of a strong electron-withdrawing group. With optimized D–A interactions of the molecules, the newly synthesized fluorophores exhibit high fluorescence quantum yields with maximized emission in the 500–600 nm region in solid state. These fluorophores were doped into PMMA to form LDS films. Applying these LDS films containing different fluorophores to the surface of a CdTe solar cell increases its power output by a magnitude of 6–10%.

The newly synthesized fluorophores (**1a–c**) are depicted in Fig. 1a. The detailed synthetic procedures and compound characterizations of these molecules are described in the ESI.† These fluorophores are designed to have TPE and malononitrile components with different aromatic rings as conjugating bridges. Our rationale is that since the malononitrile group is more electron deficient than the TPE group in the molecules, the TPE group will act as an electron donor, while the malononitrile group will act as an electron acceptor. Because of their unique D–A conjugation, we expect that these fluorophores will have both intramolecular charge transfer (ICT) and aggregation-induced emission (AIE) characteristics.

Along with the solar photon spectrum and the EQE of the CdTe solar cell modified with a 500 nm cut-off filter, Fig. 1b shows the absorption and emission spectra of these fluorophores doped in a PMMA solid film. The films were prepared as described in the Experimental section. All photophysical parameters associated with the spectra of these molecules are given in Table 1. For comparison, the photophysical properties of the commercial available fluorophore Y083 are also given in Table 1. All newly synthesized fluorophores exhibit absorption in the region below 500 nm with high absorption coefficients. The observed strong absorption is primarily attributed by the TPE group as an electron donor, which undergoes the local excited (LE) state and intramolecular charge transfer (ICT) state in the high energy (short-wavelength) region upon excitation. The emission spectra of the synthesized fluorophores show a maximum around 550 nm with high quantum yield (0.84–0.99), which is largely attributed to the malononitrile group, since the malononitrile group as the electron acceptor typically shifts the emission maximum to longer wavelength.[20] Comparing to fluorophore Y083, the synthesized fluorophores show significantly larger Stokes shifts (129–146 nm).

We hypothesize that the observed large Stokes shifts and high quantum yields are associated with the strong ICT process and AIE properties of the newly designed molecules. To test our hypothesis, we characterized both the ICT process and the AIE properties of each fluorophore. The ICT characteristics of fluorophores **1a–c** were first examined by solvatochromism measurements. Fig. 2a shows the Lippert–Mataga plots of solvatochromism measurements of the molecules. The observed Stokes shifts of all fluorophores are increased with the increase of solvent orientation polarizability: $\Delta f = (\varepsilon - 1)/(2\varepsilon + 1) - (n^2 - 1)/(2n^2 + 1)$ (Lippert–Mataga equation).[21] From the slope calculations of the solvatochromism measurements (Table S1†), we conclude that the strong ICT occurs during the excitation (absorption) and emission processes of these fluorophores when their transition dipole moment changes are larger than 20.0 D. The strong ICT characteristics of these molecules are also supported by theoretical computational studies of molecular orbital contributions to the ground and excited states using the DFT method. Our results suggested that over 60% of the charge transfer from the donor (TPE) to acceptor (malononitrile) (Table S2†) occurs during the ICT process.

The AIE properties of fluorophores **1a–c** were investigated by examining the fluorescence intensity change in acetonitrile–water mixtures (Fig. 2b). When the water fraction (f_w) is low, the fluorescence intensities of these fluorophores are very low, and when f_w rises to 60% and above, the fluorescence intensities increase significantly. This is because the molecules start to aggregate in the solvent mixture with high water content, and the molecules in the aggregated state exhibit enhanced fluorescence. The aggregation phenomenon in the solvent mixture was further investigated using fluorescence lifetime measurements. The fluorescence intensity decays of all molecules in the low f_w solvent are single-exponential with short lifetimes (1.05–1.92 ns). However, when f_w rises to 60% and above, the fluorescence intensity decays become two-exponential (Fig. S2†). One of the recovered lifetimes (1.38–2.19 ns) is associated with free fluorophores in the solution, and the other lifetime (4.32–9.43 ns) is longer than that and is associated with the aggregated fluorophores. The amplitudes associated with the longer lifetime increase with rising f_w of the solvent mixture, confirming that the observed enhanced fluorescence is indeed attributed to the aggregated fluorophores (Fig. S3†).

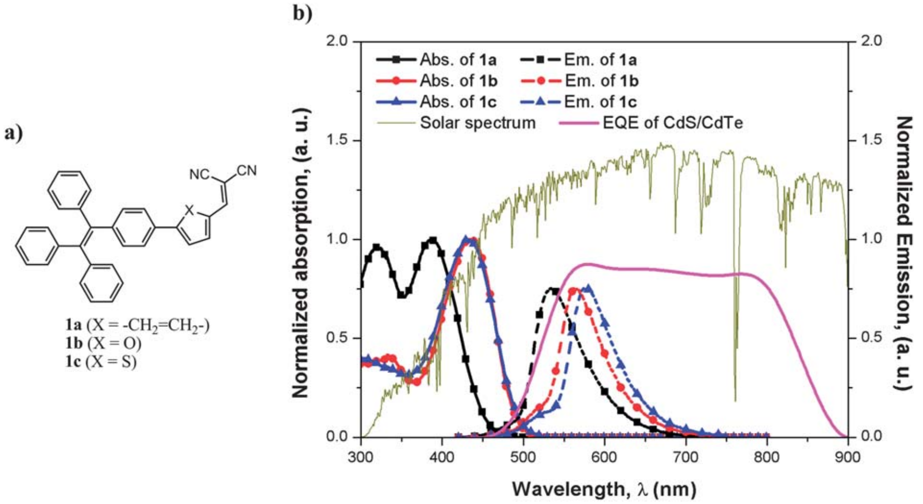

Fig. 1 (a) Molecular structures of fluorophores **1a–c**. (b) Normalized absorption (solid lines) and emission (dash lines) spectra: **1a** (λ_{ex} = 388 nm, black, ■), **1b** (λ_{ex} = 433 nm, red, ●), **1c** (λ_{ex} = 431 nm, blue, ▲) associated with AM 1.5G solar spectrum (dark yellow) and the spectral response of the modified CdTe solar cell (magenta).

Table 1 Photophysical parameters including absorption maximum (λ_{abs}), molar absorption coefficient (ε) and emission maximum (λ_{em}), Stokes shift ($\Delta\lambda = \lambda_{abs} - \lambda_{em}$), and fluorescence quantum yield (Φ_f)

Compound	λ_{abs} (nm)[a]	ε (M^{-1} cm^{-1})	λ_{em} (nm)	$\Delta\lambda$ (nm)	Φ_f[b]
1a	388	16 175	534	146	0.99
1b	433	23 168	562	129	0.93
1c	431	23 621	574	143	0.84
Y083	476	19 785	540	64	0.92

[a] Lower energy absorption maximum. [b] Relative value to Y083.

The thermal properties of all fluorophores were also investigated by thermogravimetric analysis (TGA) and differential scanning calorimetry (DSC) (Fig. S4†). The decomposition temperature is defined at 5% of mass loss. Fluorophore **1a** decomposes at 132 °C before melting while fluorophores **1b** and **1c** decompose at higher temperatures of 291 °C and 245 °C, respectively, suggesting that both fluorophores **1b** and **1c** are highly thermally stable in air. It is worth noting that fluorophore **1c** shows no phase change in DSC measurements, whereas fluorophore **1b** melts at 239 °C. This may due to the thiophene group that stabilizes the whole conjugated system.[22]

Photonic characterizations of these synthesized molecules provide a basis for us to investigate the potential application of these fluorophores as LDS materials in CdTe solar energy harvesting. As mentioned earlier, the LDS solid films containing these fluorophores were prepared by doping 0–0.8% (w/w%) of each fluorophore in PMMA. Y083 doped PMMA solid films were used as the reference in this study. The average thickness of these solid films is about 85 μm and typical absorption and emission spectra of these fluorophores doped in the LDS films are shown in Fig. 1b. The LDS effect of the fluorophore-doped PMMA films on solar energy conversion of the CdTe solar cell was examined by placing the LDS films on the cell surface and monitoring the increase of the current outputs. As expected, the current outputs of the CdTe solar cell significantly increased in response to each synthesized fluorophore doped in LDS films.

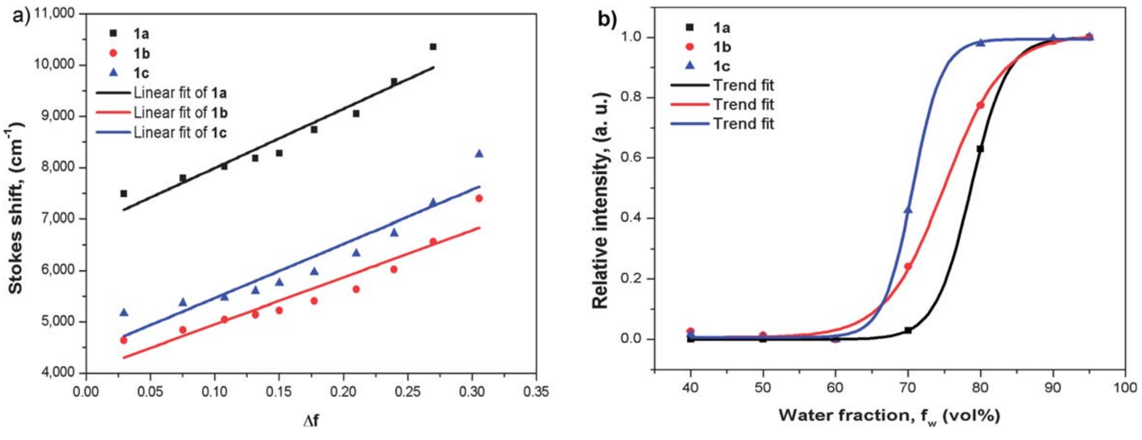

Fig. 2 (a) Lipper–Mataga plots of solvatochromism measurements. (b) AIE properties in acetonitrile–water mixtures. Fluorophore concentration is 15 μM.

Fig. 3a shows the increase of the short circuit current density (J_{sc}) of the CdTe solar cell with the increase of the doped concentrations of each fluorophore in the LDS films. Fluorophore **1a** exhibits 6% of maximum increase of J_{sc}, which is lower than the reference Y083 (8%), due to its absorption spectral mismatch with the solar spectrum in the region below 500 nm and emission spectral mismatch with the bandgap of the CdTe solar cell in the region over 500 nm (Fig. 1b). Fluorophores **1b** and **1c** exhibit 10% and 9% of maximum increase of J_{sc}, respectively, which is higher than the reference of Y083, because of improved absorption and emission spectral matches of these two fluorophores. The enhanced spectral response of the CdTe solar cell in the short-wavelength region (<500 nm) was also verified by measuring the EQE of the CdTe solar cell with LDS films (Fig. 3b). These results suggest that the LDS films containing our synthesized fluorophores efficiently absorb short-wavelength photons (<500 nm) and re-emit photons at wavelengths (>500 nm) above the bandgap of the CdS layer, therefore improving the solar harvest efficiency of the cell. However, due to the photon escape at the film surface (~12.5%)[23,24] and the photon side loss (~8.2%)[25] at the film edge as well as other experimental factors, the resulting 10% of maximum increase of J_{sc} is far lower than the expected 20% theoretical maximum increase for the CdTe solar cell under the AM 1.5G spectrum based on our experimental setup.[26] Even so, it is still significant to see the 10% maximum increase in the J_{sc} of the CdTe solar cell by using novel AIE fluorophores as LDS materials because this may pave a new path for developing effective LDS materials in the future.

In conclusion, in this work, a new type of TPE-based fluorophore is synthesized and applied as an LDS material for improving the solar energy conversion of a CdTe solar cell. In contrast to the conventional TPE-based fluorophores in which TPE is typically used as an electron acceptor, in our molecular design the TPE is paired with a malononitrile group and utilized as an electron donor. This novel design effectively overcomes some photonic drawbacks associated with most of the TPE-based AIE fluorophores that prevent them from being used as LDS materials for solar cell applications. The success of our design is that the newly synthesized fluorophores take the advantage of both ICT and AIE, which leads to enlarged Stokes shift and high quantum yield in solid medium. With these desired photonic properties, these fluorophores significantly improve the spectral response of the CdTe solar cell to the short-wavelength photons (<500 nm) when they are doped in PMMA films as LDS materials. Ultimately, the measured short circuit current density (J_{sc}) of the CdTe solar cell is significantly increased by a magnitude of 6–10% when the PMMA films containing each fluorophore are applied to the surface of the cell. Currently, active work in our lab is in progress to develop more efficient LDS materials for photovoltaic cell applications based on this new molecular design strategy.

Experimental

LDS films were prepared by following the procedure developed in our lab. Briefly, 7.5 g of PMMA powder (purchased from TCI America) was dissolved in 100 g of toluene in a 250 mL flask. The mixture was stirred overnight and the insoluble PMMA was filtered off. Then, 5 g of the PMMA solution was mixed with variable amounts of each of the synthesized fluorophores in a 10 mL vial. The fluorophore/PMMA solution was poured into a Petri dish (R25 × 15 mm). The solvent was evaporated under ambient conditions and further removed in a vacuum oven for 1 h. The films were finally cut and peeled off from the Petri dish in warm water.

Absorption spectra were recorded with a Beckman Coulter DU730 Life Science UV-Vis spectrophotometer at room temperature. Emission spectra were collected on an ISS PC1 photon counting spectrofluorometer at 20 °C. Fluorescence

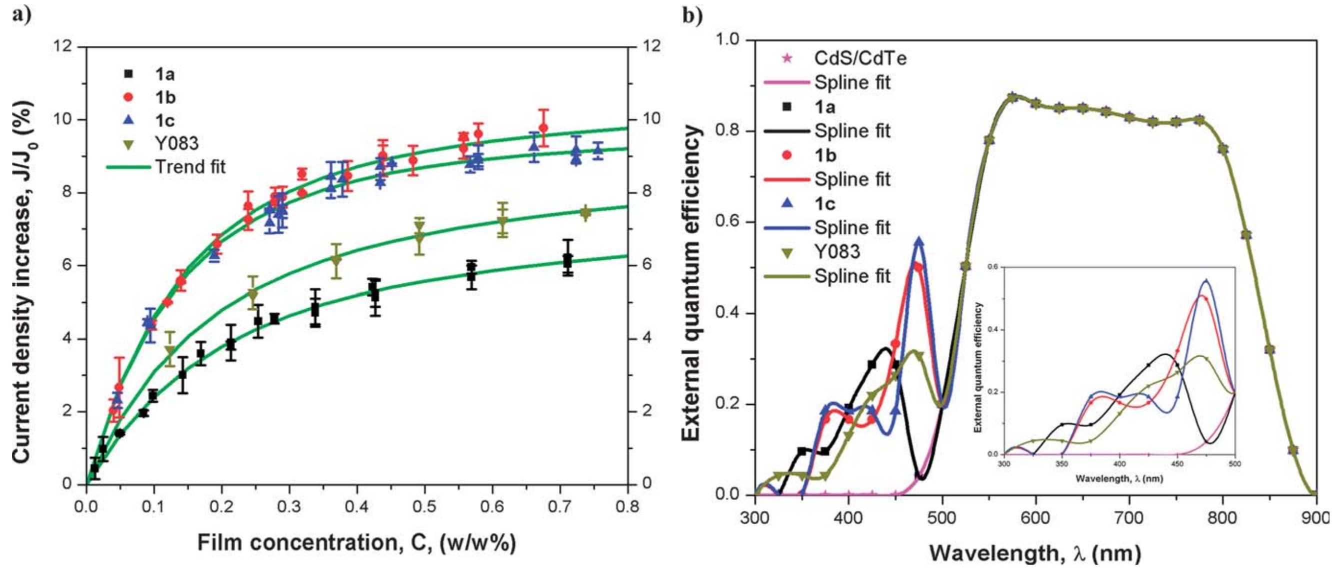

Fig. 3 (a) The increase of short circuit current density (J_{sc}) *vs.* the different concentrations of the LDS film placed on the CdTe solar cell surface for fluorophores **1a–c** and Y083. (b) Enhanced spectral response at short-wavelengths after the LDS film was placed on the CdTe solar cell surface for fluorophores **1a–c** and Y083.

lifetimes were measured on a HORIBA JOBIN YVON fluorocube using 459 nm LED as the excitation light source with a 500 nm long pass filter at room temperature.

Theoretical calculations were conducted using the Gaussian 09 package.[27] All fluorophores were calculated under the gas phase without using the SCRF method to reduce the computational effort. Ground state (S_0) geometries were optimized using the B3LYP/6-311G(d) function. Excited state (S_1) geometries were optimized using the time-dependent (TD) method with the same function. Single point calculations were conducted at the S_0 and S_1 optimized geometries.

Thermal stabilities were studied on PerkinElmer TGA 7 and DSC 7. TGA analysis was performed under ambient conditions from 30 °C to 400 °C at a rate of 10 °C min^{-1}. The typical mass used for DSC runs was 3.0–3.5 mg. The scans were performed from 30 °C to 340 °C at a rate of 10 °C min^{-1}.

In the LDS measurements, a 150 W solar simulator (model# 96000, Newport Corporation) with an AM 1.5G filter (model# 81092, Newport Corporation) was used as the light source. The spectral response of the magnetron sputtered CdTe solar cell[28] was modified by a 500 nm long pass filter to achieve the EQE in Fig. 1. The filter was used to emphasize the effect of the LDS material. The interface between the solid film and the surface of the solar cell was filled with index matching fluid to minimize the refraction of the air. The detailed LDS measurements are given in ESI,† Section 8.

References

1 A. Luque and S. Hegedus, *Handbook of Photovoltaic Science and Engineering*, John Wiley & Sons, Ltd, NJ, USA, 2003.

2 D. H. Rose, F. S. Hasoon, R. G. Dhere, D. S. Albin, R. M. Ribelin, X. S. Li, Y. Mahathongdy, T. A. Gessert and P. Sheldon, *Prog. Photovolt.: Res. Appl.*, 1999, **7**, 331–340.

3 E. Klampaftis, D. Ross, K. R. McIntosh and B. S. Richards, *Sol. Energy Mater. Sol. Cells*, 2009, **93**, 1182–1194.

4 X. Huang, S. Han, W. Huang and X. Liu, *Chem. Soc. Rev.*, 2013, **42**, 173–201.

5 L. Danos, T. Parel, T. Markvart, V. Barrioz, W. S. M. Brooks and S. J. C. Irvine, *Sol. Energy Mater. Sol. Cells*, 2012, **98**, 486–490.

6 E. Klampaftis, D. Ross, S. Seyrling, A. N. Tiwari and B. S. Richards, *Sol. Energy Mater. Sol. Cells*, 2012, **101**, 62–67.

7 D. Ross, E. Klampaftis, J. Fritsche, M. Bauer and B. S. Richards, *Sol. Energy Mater. Sol. Cells*, 2012, **103**, 11–16.

8 R. Ferrini, O. Nicolet, S. Huber, L. Zuppiroli, S. Chappellet, C. Lovey, J. Perrenoud and M. Pauchard, *J. Appl. Phys.*, 2010, **107**, 114323.

9 B. S. Richards and K. R. McIntosh, *Prog. Photovoltaics*, 2007, **15**, 27–34.

10 Y. Hong, J. W. Y. Lam and B. Z. Tang, *Chem. Soc. Rev.*, 2011, **40**, 5361–5388.

11 Y. N. Hong, J. W. Y. Lam and B. Z. Tang, *Chem. Commun.*, 2009, 4332–4353.

12 Y. Liu, S. M. Chen, J. W. Y. Lam, P. Lu, R. T. K. Kwok, F. Mahtab, H. S. Kwok and B. Z. Tang, *Chem. Mater.*, 2011, **23**, 2536–2544.

13 Y. Liu, S. M. Chen, J. W. Y. Lam, F. Mahtab, H. S. Kwok and B. Z. Tang, *J. Mater. Chem.*, 2012, **22**, 5184–5189.

14 Z. J. Zhao, C. Y. K. Chan, S. M. Chen, C. M. Deng, J. W. Y. Lam, C. K. W. Jim, Y. N. Hong, P. Lu, Z. F. Chang, X. P. Chen, P. Lu, H. S. Kwok, H. Y. Qiu and B. Z. Tang, *J. Mater. Chem.*, 2012, **22**, 4527–4534.

15 J. R. Lakowicz, *Principles of Fluorescence Spectroscopy*, Springer Science+Business Media, NY, USA, 3rd edn, 2006.

16 W. Qin, D. Ding, J. Z. Liu, W. Z. Yuan, Y. Hu, B. Liu and B. Z. Tang, *Adv. Funct. Mater.*, 2012, **22**, 771–779.

17 W. Z. Yuan, Y. Y. Gong, S. M. Chen, X. Y. Shen, J. W. Y. Lam, P. Lu, Y. W. Lu, Z. M. Wan, R. R. Hu, N. Xie, H. S. Kwok, Y. M. Zhang, J. Z. Sun and B. Z. Tang, *Chem. Mater.*, 2012, **24**, 1518–1528.

18 Q. L. Zhao, K. Li, S. J. Chen, A. J. Qin, D. Ding, S. Zhang, Y. Liu, B. Liu, J. Z. Sun and B. Tang, *J. Mater. Chem.*, 2012, **22**, 15128–15135.

19 Y. L. Li, L. Scudiero, T. H. Ren and W. J. Dong, *J. Photochem. Photobiol., A*, 2012, **231**, 51–59.

20 Y. Li, T. Ren and W.-J. Dong, *J. Photochem. Photobiol., A*, 2013, **251**, 1–9.

21 F. B. Dias, S. Pollock, G. Hedley, L. O. Palsson, A. Monkman, I. I. Perepichka, I. F. Perepichka, M. Tavasli and M. R. Bryce, *J. Phys. Chem. B*, 2006, **110**, 19329–19339.

22 R. Kerner, Y. L. Li and L. Scudiero, *Synth. Met.*, 2012, **162**, 1198–1203.

23 H. J. Hovel, R. T. Hodgson and J. M. Woodall, *Sol. Energy Mater.*, 1979, **2**, 19–29.

24 W. Viehmann, *Meas. Opt. Radiat.*, 1979, **196**, 90–95.

25 G. C. Glaeser and U. Rau, *Thin Solid Films*, 2007, **515**, 5964–5967.

26 American Society for Testing and Materials, Solar spectral irradiance standard curves, international standard curve for terrestrial global air mass 1.5 ASTM G173-03. http://rredc.nrel.gov/solar/spectra/am1.5/, 2003 (accessed 23.03.2013).

27 M. J. Frisch, G. W. Trucks, H. B. Schlegel, G. E. Scuseria, M. A. Robb, J. R. Cheeseman, G. Scalmani, V. Barone, B. Mennucci, G. A. Petersson, H. Nakatsuji, M. Caricato, X. Li, H. P. Hratchian, A. F. Izmaylov, J. Bloino, G. Zheng, J. L. Sonnenberg, M. Hada, M. Ehara, K. Toyota, R. Fukuda, J. Hasegawa, M. Ishida, T. Nakajima, Y. Honda, O. Kitao, H. Nakai, T. Vreven, J. A. Montgomery, Jr, J. E. Peralta, F. Ogliaro, M. Bearpark, J. J. Heyd, E. Brothers, K. N. Kudin, V. N. Staroverov, R. Kobayashi, J. Normand, K. Raghavachari, A. Rendell, J. C. Burant, S. S. Iyengar, J. Tomasi, M. Cossi, N. Rega, J. M. Millam, M. Klene, J. E. Knox, J. B. Cross, V. Bakken, C. Adamo, J. Jaramillo, R. Gomperts, R. E. Stratmann, O. Yazyev, A. J. Austin, R. Cammi, C. Pomelli, J. W. Ochterski, R. L. Martin, K. Morokuma, V. G. Zakrzewski, G. A. Voth, P. Salvador, J. J. Dannenberg, S. Dapprich, A. D. Daniels, O. Farkas, J. B. Foresman, J. V. Ortiz, J. Cioslowski, and D. J. Fox, *Gaussian 09, Revision. A.01*, Gaussian, Inc., Wallingford CT, 2009.

28 A. Gupta and A. D. Compaan, *Appl. Phys. Lett.*, 2004, **85**, 684–686.